



HAL
open science

Development of porosimetry techniques for the characterization of plasma-treated porous ultra low-K materials

Christophe Licitra, Thierry Chevolleau, Régis Bouyssou, Mohamed El Kodadi, Georg Haberfehlner, Jérôme Hazart, Leopold Virost, Maxime Besacier, Nicolas Possémé, Maxime Darnon, et al.

► **To cite this version:**

Christophe Licitra, Thierry Chevolleau, Régis Bouyssou, Mohamed El Kodadi, Georg Haberfehlner, et al.. Development of porosimetry techniques for the characterization of plasma-treated porous ultra low-K materials. ECS Transactions, 2011, 35 (4), pp.729-746. 10.1149/1.3572316 . hal-00625361

HAL Id: hal-00625361

<https://hal.science/hal-00625361>

Submitted on 13 Dec 2022

HAL is a multi-disciplinary open access archive for the deposit and dissemination of scientific research documents, whether they are published or not. The documents may come from teaching and research institutions in France or abroad, or from public or private research centers.

L'archive ouverte pluridisciplinaire **HAL**, est destinée au dépôt et à la diffusion de documents scientifiques de niveau recherche, publiés ou non, émanant des établissements d'enseignement et de recherche français ou étrangers, des laboratoires publics ou privés.

Development of Porosimetry Techniques for the Characterization of Plasma-Treated Porous Ultra Low- k Materials

C. Licitra^a, T. Chevolleau^b, R. Bouyssou^b, M. El Kodadi^b, G. Haberfehlner^a, J. Hazart^a, L. Viro^a, M. Besacier^b, N. Posseme^a, M. Darnon^b, R. Hurand^b, P. Schiavone^b, and F. Bertin^a

^aCEA-LETI, Minatec Campus, 17 rue des Martyrs, 38054 Grenoble, France

^bLTM, UJF-Grenoble1/Grenoble-INP/CNRS/CEA, Minatec Campus, 17 rue des Martyrs, 38054 Grenoble, France

For the sub-32 nm node, porous SiCOH dielectrics (p-SiCOH) are integrated using dual damascene patterning by etching trenches and vias into the porous material. One challenge is to control the process conditions to minimize the plasma-induced damage of p-SiCOH materials at the bottom and at the sidewall of the trenches. Ellipsometric Porosimetry has been adapted to characterize the plasma-treated materials for both horizontal and vertical surfaces. Since surface modifications can cause adsorption and desorption delays and hydrophobicity loss, porosimetry measurements operated with multi-solvent and kinetic protocols are required. Quantitative measurements of vertically patterned materials are demonstrated using periodic structures of porous material and a Scatterometric Porosimetry analysis. Results show a good sensitivity of the measurement to the different process conditions but also highlight a different impact of the plasma processes on patterned materials compared with blanket films.

Introduction

Down-scaling of complementary metal oxide semiconductor (CMOS) devices requires the integration of copper/porous ultra low- k (ULK) materials to reduce the interconnect resistance-capacitance delay. For the sub-32 nm node, porous SiCOH dielectrics (p-SiCOH) are integrated using dual damascene patterning by etching trenches and vias into the porous material (Figure 1). Since the pore structure leads to higher sensitivity of the material to environmental and process conditions, controlling the profiles of the etched structures and minimizing the plasma-induced damage of p-SiCOH materials are the two main patterning challenges. The sensitive areas are the bottom and the sidewall of the trenches where surface modifications, post-etch residues, or p-SiCOH roughening can occur (1, 2, 3). Characterization techniques with low spatial resolution including X-ray Photoelectron Spectroscopy, X-ray Reflectivity, Time of Flight - Secondary Ion Mass Spectrometry, Contact Angle, Mercury Probe Capacitance, Infrared Spectroscopy, or Ellipsometric Porosimetry can be easily set up on blanket films to replicate the bottom of the trench (1). Unfortunately the porous properties of the sidewall region differ from the bottom of the trench. Few studies have been performed on patterned structures to determine the sidewall modification while this information is critical for device performance (4). In this study, Ellipsometric Porosimetry (EP) has been adapted to characterize the plasma-treated materials for both horizontal and vertical geometries. EP

is a non destructive technique (5) based on the acquisition of ellipsometric spectra of a layer during the adsorption and desorption cycles of an adsorptive (solvent). However, it can suffer from measurement artifacts when used with plasma-treated films because of surface modifications. We have therefore evaluated different experimental configurations. Results show that using solvents with different molecular diameters, e.g. toluene and methanol, allows surface densification to be detected. This plasma-sealing effect can also be quantified by studying the solvent penetration kinetics over time through the damaged surface. Finally for hydrophobic materials, the plasma-induced degree of hydrophilization of the surface can also be determined through EP with water vapors. On the other hand, the properties of vertical sidewalls can be determined using the recently developed Scatterometric Porosimetry (SP) technique (6, 7). It mainly consists in the use of the EP tool to record the scatterometric response of periodic structures made of porous material as a function of the relative pressure of the solvent. The patterned structures are chosen to have a critical dimension (CD) which is equivalent to the dielectric line size of the interconnect except that they typically consist of parallel periodic lines. The porous properties are subsequently extracted from the SP measurement with the use of a specially-developed scatterometric modeling. We show a side-by-side comparison between EP and SP on different plasma-treated samples. A different effect of the plasma processes is observed on patterned materials compared with blanket films. These results illustrate that the porous material modifications strongly depend on the sample geometry and highlight the interest of Scatterometric Porosimetry to characterize sidewall damage after each step of the etch process.

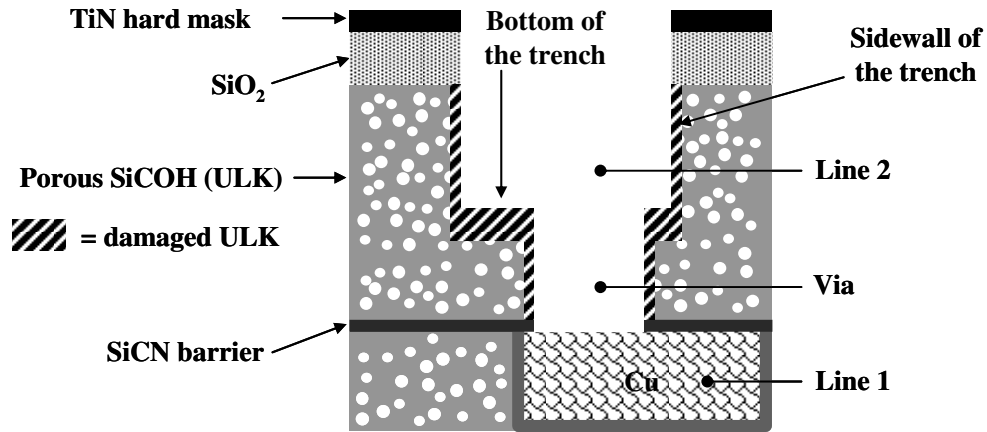


Figure 1. Dual damascene structure fabricated using a metallic hard mask.

Experimental Details

Integration process

Porous SiCOH films with a thickness around 120 nm were deposited by Plasma Enhanced Chemical Vapor Deposition on blanket 300 mm silicon wafers. The material is the BD2.35TM from Applied Materials with $k=2.35$, 28 % porous, 1.2 nm mean pore radius and hydrophobic by design. Porosity is achieved by co-depositing two precursors to make a SiCOH skeleton containing organic species which are subsequently removed using an ultraviolet assisted thermal cure at 400°C. In order to simulate the integration process, porous blanket films were etched in conventional fluorocarbon based plasmas ($CF_4 / C_4F_8 / N_2 / Ar$) and after partial etching the remaining films was exposed to post-etching treatments such as NH_3 , H_2 , CH_4 or O_2 based plasmas (8). The etching and post-

etching plasma treatments were performed in a dual frequency capacitive discharge Flex45DD™ from Lam Research.

On the other hand, the patterning of porous ULK lines was performed using a dual metallic hard mask strategy. This architecture is mainly used to minimize the porous dielectric exposure to environmental contamination and to stripping plasmas. A simplified stack was used to replicate the dual damascene vertical structures. It consists of a 15 nm titanium nitride layer, a 125 nm oxide capping layer, and the BD2.35™ p-SiCOH dielectric material ~600 nm thick. In the visible range, the 15 nm titanium nitride layer is transparent allowing optical measurements through the layer. After lithography, the TiN hard mask patterning step was performed in inductively coupled plasma using chlorine-based chemistries while the SiO₂ capping and the p-SiCOH layers were etched in fluorocarbon-based plasmas using a capacitive coupled plasma (Flex45DD™). After patterning, porous structures were also exposed to NH₃, H₂, CH₄, or O₂ based plasmas. A Scanning Electron Microscopy (SEM) image of such a patterned structure is shown in Figure 2 after the etching process steps.

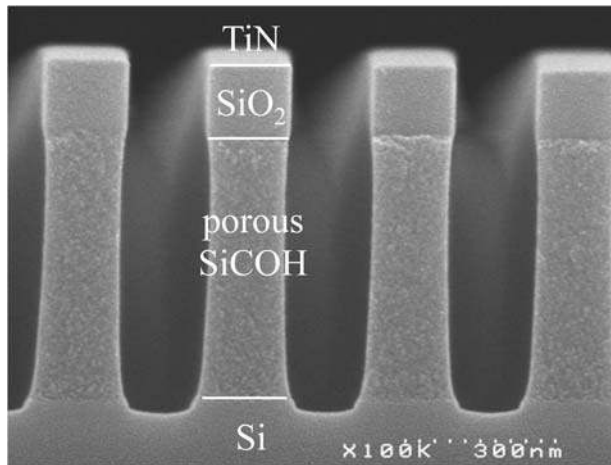


Figure 2. Test structure for Scatterometric Porosimetry with critical dimension CD=180 nm and pitch=340 nm.

Characterization tool

EP and SP measurements are performed in the visible range on an ellipsometric porosimeter from SOPRALAB (SEMILAB). It consists of a rotating polarizer spectroscopic ellipsometer coupled with a vacuum chamber which is operated at a pressure ranging from 0.133 Pa to the saturation vapor pressure (P_s) of the adsorptive (Figure 3) to allow capillary condensation into the open pores. Three solvents were separately used as adsorptive: toluene ($P_s \sim 3333$ Pa at room temperature, refractive index at 633 nm $n_{tol} = 1.492$), methanol ($P_s \sim 14000$ Pa at room temperature, refractive index at 633 nm $n_{met} = 1.329$) and water ($P_s \sim 2666$ Pa, $n_{water} = 1.333$ at 633 nm). Pressure values are plotted using a relative scale $P_{rel} = P/P_s$, with P the chamber pressure. The standard porosimetry cycle consists of an adsorption sequence ($P_{rel} = 0$ to 1) followed by a desorption sequence ($P_{rel} = 1$ to 0) which are called isotherms, but measurements can also be done as a function of time at fixed pressures. In our experiments the dwell time for each pressure step is less than 1 min for measurements over pressure and time interval is set to 5 s for measurements over time. For each step, ellipsometric spectra are recorded at an incidence angle of 60.15°, in a typical wavelength range between 1.5 and 4 eV using a

multichannel detector. More details about the experimental setup and EP technique can be found elsewhere (9, 10).

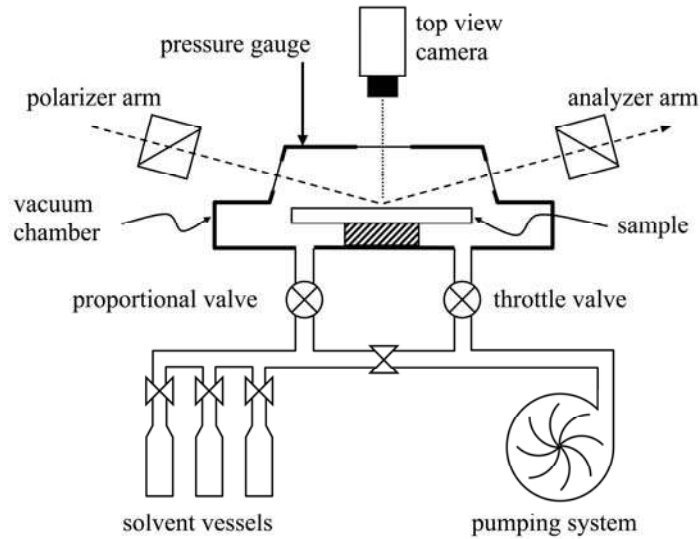


Figure 3. Ellipsometric porosimeter setup.

Data modeling

The experimental data acquired with the SOPRALAB system are the ellipsometric coefficients of the sample: $\tan(\Psi)$ and $\cos(\Delta)$ or α and β as a function of photon energy and relative pressure. These coefficients can be used with an ellipsometric modeling to determine the thickness and the optical properties of the porous film in the form of the complex refractive index $N=n+ik$ at each pressure step. If the sample is a patterned structure instead of a thin film, scatterometry must be used to model α and β coefficients. Scatterometry is a non-destructive optical method that allows the geometry of a periodic structure such as a grating to be determined by modeling its optical diffracted response (11). It is usually applied to materials with fixed refractive index. However we have adapted the scatterometric analysis to extract the properties of porous gratings by modeling the optical index variations of the porous material during the adsorption and desorption sequences. Since a real circuit cannot be properly modeled directly, specific periodic structures made of porous materials were used to replicate the interconnect levels that need to be characterized. These gratings can be chosen to have a critical dimension which is equivalent to the interconnect line size except that they typically consist of parallel periodic lines. This kind of structures can usually be found into the service areas of the photomasks or can be prepared specifically using the same process as for the interconnect levels manufacturing. α and β coefficients of the grating depend on its geometry including the CD, height, side wall angle; the periodicity of the lines; and on the optical indices of all component materials. During the optical measurement we used the standard scatterometry configuration where the periodic lines are placed perpendicular to the plane of incidence of the light beam. An example of EP and SP measurements is given in Figure 4. Because of refractive index variations, we observe a shift of the $\tan(\Psi)$ and $\cos(\Delta)$ spectra while the p-SiCOH is being filled with methanol.

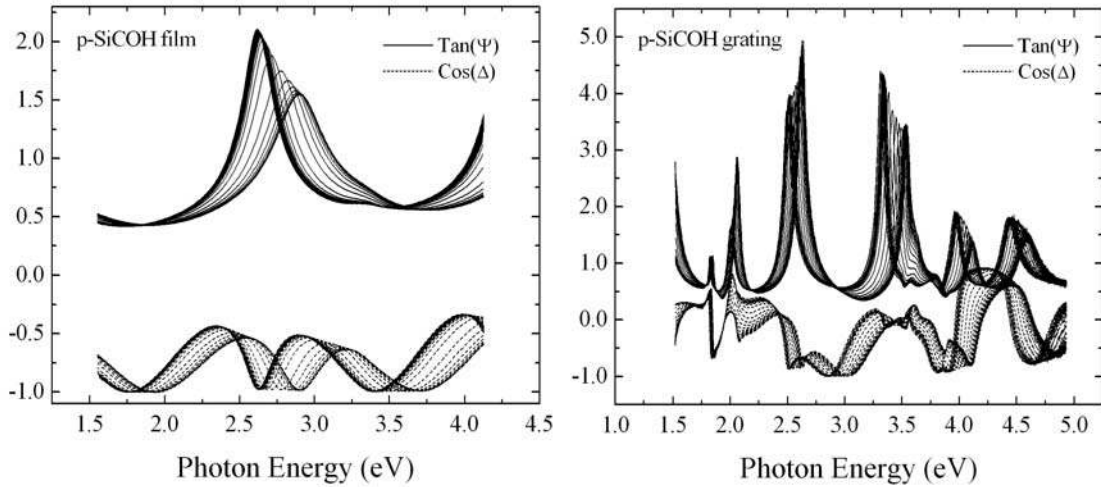


Figure 4. $\tan(\Psi)$ and $\cos(\Delta)$ spectra during methanol adsorption. Left: porous film, right: porous grating.

During the porosimetry cycle the effective refractive index of the porous material partially filled with solvent must be modeled at each relative pressure. Absorbance measurements were performed using a Cary 5 spectrophotometer from Varian through 1 cm of liquid toluene, methanol and deionized water to ensure that no absorption peak from the solvent should be included in the porous material refractive index (Figure 5, left). A 130 nm p-SiCOH film was also measured after deposition using a broad range M2000 spectroscopic ellipsometer from Woollam. This type of dielectric material shows several absorption peaks in the ultraviolet region as depicted in Figure 5, right. However within the restricted EP spectral range the p-SiCOH refractive index can be modeled using classical dispersion laws such as Tauc-Lorentz, Forouhi-Bloomer or Cauchy law with a Lorentz oscillator. Each of these laws has 5 variable parameters. In this study we chose a Cauchy law with a Lorentz oscillator to easily model the p-SiCOH refractive index by adjusting only 2 Cauchy parameters during the condensation. Indeed the solvents extinction coefficients calculated from the absorbance spectra are lower than 10^{-7} thus the Lorentz oscillator which takes into account the porous material absorption can remain constant during the adsorption and desorption sequences.

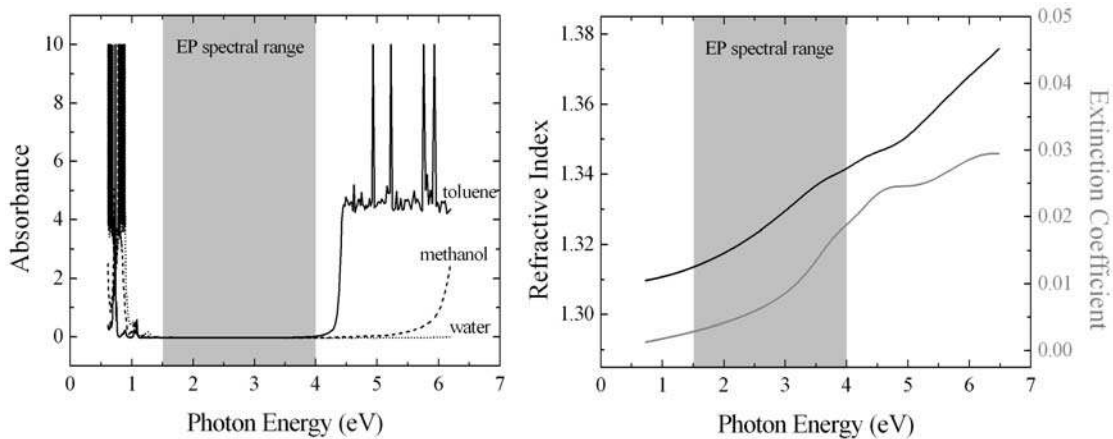


Figure 5. Left: absorbance spectra through 1 cm of liquid toluene, methanol and deionized water. Right: refractive index and extinction coefficient of an as-deposited porous SiCOH film after curing.

EP or SP porosimetry modeling then consists in fitting all the spectra recorded as a function of photon energy and relative pressure. On one hand, the ellipsometric simulated signatures of blanket films can be easily derived from the reflection coefficients of the p- and s-polarized waves known as Fresnel equations (12). On the other hand, the simulated signatures of a grating are obtained using a rigorous electromagnetic solver based on the Modal Method by Fourier Expansion (MMFE) detailed by Li et al. (13). The MMFE method uses a modal decomposition of Maxwell's equations with appropriate boundary conditions at each interface of the geometric structure to solve the electric field in each region of the sample. The simulation of the optical signatures is known as the direct problem. In order to model the experimental data versus photon energy, a minimization algorithm such as the least-squares algorithm can be used. This optimization is commonly employed for ellipsometry and for EP data analysis. The least-squares can be used for SP modeling but it is also possible to apply a faster library-based method to model the optical response of the grating. First a library of optical responses is built by mapping the optical indices of the porous material and the variable geometric parameters of the sample including CD, height, side wall angle or other required parameters. Then the experimental signatures are compared to the library to quickly find the unknown parameters. This method is widely used for in-line scatterometry with fixed refractive indices and for real-time scatterometry (14). Both the least-squares and the library-based minimization techniques were tried to model SP measurements and gave similar results. The modeling of the optical responses versus pressure can be done in different manners. We have tested the 3 following modeling strategies.

Sequential strategy. This technique is commonly used for EP data analysis with commercially available software. A first ellipsometric or scatterometric modeling step is used to calculate the optical indices and the geometric parameters: thicknesses in the case of a blanket stack or geometry of the grating including CD, height, side wall angle or other required parameters. This calculation is done on the first measurement corresponding to the vacuum state when no pores are filled. The optical indices of each material should preferably be determined on blanket wafers to get a robust initial model. A sequential modeling step with less variable parameters is then applied to calculate the p-SiCOH refractive index variations during the adsorption or desorption of the adsorptive. During this step the geometry can be kept constant or also fitted if necessary. As the solvent doesn't absorb light in the visible range only the two Cauchy parameters are sequentially fitted. The optical indices of each non porous material are kept constant.

Reversed sequential strategy. This modeling is a sequential strategy but the refractive indices and the geometric parameters are determined at relative pressure $P_{rel}=1$ instead of $P_{rel}=0$ and the sequential fit is done in the reversed order from $P_{rel}=1$ to 0.

Combined strategy. The sequential strategies can lack of precision when some parameters are correlated. We have therefore adapted our minimization algorithm to the specificity of porosimetry experiments. Indeed EP and SP measurements contain redundant information because multiple measurements are done at the same location. In some cases this information can be used to reduce the modeling errors because several model parameters are constant with pressure. Usually the optical indices of each non porous material, the Lorentz peak, and potentially some geometric parameters are fixed especially for SP. In the combined strategy these fixed parameters are no longer determined under vacuum only but by fitting measurements at several relative pressures

simultaneously (usually up to 5 pressures at once). This guarantees that these parameters are fitted to achieve a low modeling error over the whole pressure range. After this first combined fit the parameters varying with pressure that is to say the 2 Cauchy parameters and some varying geometric parameters are then fitted sequentially at each pressure.

For both EP and SP the fraction of solvent adsorbed in the pores is finally calculated at each relative pressure with the Lorentz-Lorenz effective medium approximation (15) and by knowing the effective refractive index of the material and the refractive index of condensed solvent at 633 nm (9). The open porosity is given by the solvent volume fraction when the relative pressure is equal to 1 and all open pores are filled with solvent. Finally the pore size distribution (PSD) of mesopores, $1 \text{ nm} < \text{radius} < 25 \text{ nm}$, can be calculated using the Kelvin equation of capillary condensation (16, 17) and by knowing the thickness of the layer of solvent condensed on the pore walls before capillary condensation occurs.

An example of different EP modeling strategies is given in Figure 6 (left) for methanol adsorption in a 130 nm blanket porous SiCOH film. In the case of the combined strategy only the Lorentz oscillator was simultaneously fitted at different relative pressures distributed over the range. The mean square error (Chi^2) extracted from the modeling is shown as a function of the relative pressure for the different strategies. As expected we observe that Chi^2 is lower at $P_{rel}=0$ for the sequential fit and lower at $P_{rel}=1$ for the reversed sequential fit. However the combined fit shows a relatively low average Chi^2 over the whole pressure range. The corresponding solvent volume fraction is shown in Figure 6 (right). The open porosity varies from 25.3% to 26.1% depending on the modeling. This can be attributed to parameter correlation between the thickness and the refractive index.

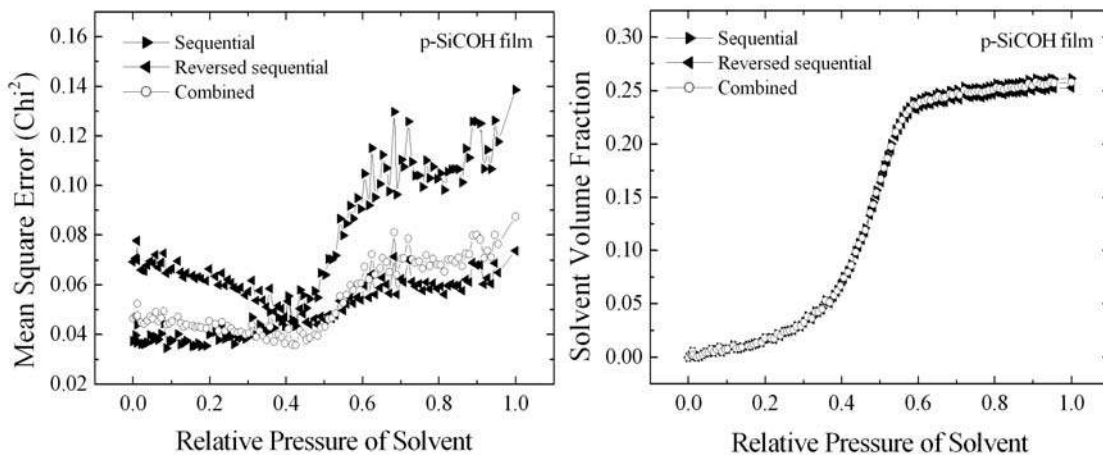


Figure 6. Left: mean square error for different modeling strategies of a 130 nm blanket porous SiCOH film. Right: corresponding solvent volume fractions for the different modeling strategies.

The same modeling strategies were applied to the porous grating shown in Figure 2. In the case of the combined strategy, the Lorentz oscillator and the geometric parameters were all simultaneously fitted at different relative pressures distributed over the range. For the 2 sequential strategies, the geometric parameters were fixed to lower the correlations between parameters. Mean square errors and solvent volume fractions are

shown in Figure 7. As the geometry was fixed at $P_{rel}=0$ the 2 sequential strategies results are very close meaning that the Lorentz parameters were found identical at $P_{rel}=0$ and $P_{rel}=1$. However the Chi^2 is high at saturation pressure. On the contrary, the combined modeling allows the Chi^2 to be lowered over the whole pressure range. As scatterometry modeling has more parameters than ellipsometry, this strategy is therefore interesting to lower the correlations between the parameters especially when fitting the geometric parameters of the structure.

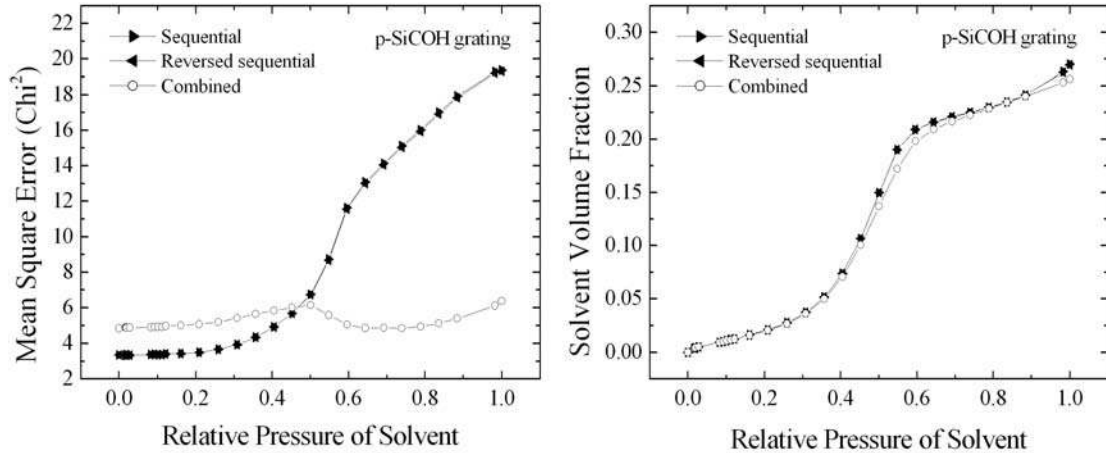


Figure 7. Left: mean square error for different modeling strategies of a porous grating. Right: corresponding solvent volume fractions for the different modeling strategies.

Results and Discussion

Effect of plasma processes on blanket p-SiCOH films

After patterning, the p-SiCOH can be exposed to NH_3 , H_2 , CH_4 , or O_2 based plasmas. Such reducing and oxidizing treatments can be used as i) ashing processes (1), ii) cleaning processes after etching, and/or iii) plasma processes to prevent the metallic barrier diffusion (18). Unfortunately they can also lead to surface modifications that can cause the formation of a damaged surface layer (1, 18, 19, 20) and increase the ULK effective dielectric constant. Indeed the damaged surface may present a barrier-like effect because of the densification of the material. The p-SiCOH which is hydrophobic by design can also become partly hydrophilic after plasma treatments because of a methyl group depletion converting the surface layer into a hydrophilic material. Figure 8 shows the water isotherms obtained with EP of an as-deposited p-SiCOH film compared to a film after exposure to O_2 downstream plasma ($k=2.5$ and 25% porosity in that case). The O_2 downstream plasma is known to remove all the methyl groups of the ULK leading to a fully hydrophilic material (1). Indeed no water adsorption is detected for the as-deposited film whereas 24.7% of the material is hydrophilic after the O_2 downstream plasma which is almost the total initial open porosity.

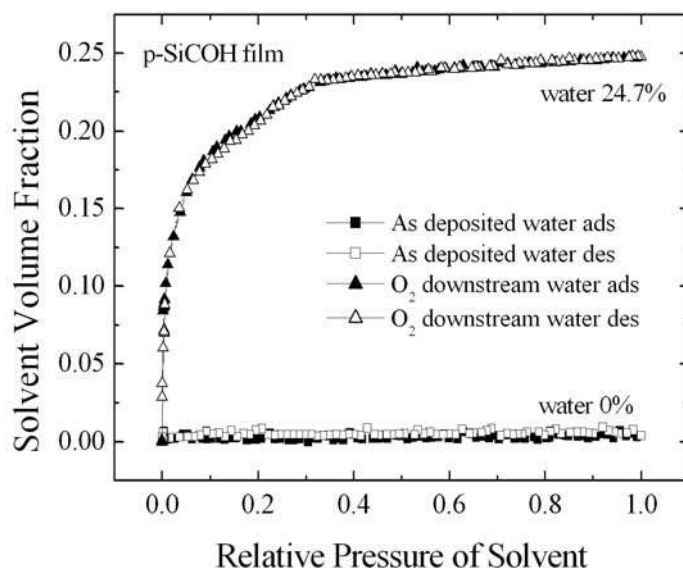


Figure 8. Water isotherms of as-deposited and O₂ downstream post-treated p-SiCOH films.

In contrast to the O₂ downstream plasma, the p-SiCOH film is partially modified after exposure to the different post-etching treatments. The modified layers can be etched in HF solution whereas the pristine hydrophobic material cannot (21). The thicknesses of the modified layers were therefore estimated by measuring the samples before and after HF etching using spectroscopic ellipsometry (Table I). After exposure to the different plasmas, dielectric constant measurements were performed on blanket wafers using a mercury probe capacitance measurement system. As expected, all the treatments lead to an increase of the dielectric constant (Table I) which is linked to the modification of the surface layer.

TABLE I. Dielectric constant and surface properties of p-SiCOH blanket samples.

Porous films	Dielectric constant	Modified layer thickness (nm)
ULK (pristine)	2.35±0.05	0
ULK+etch	2.76±0.05	28
ULK+etch+NH ₃	2.98±0.05	28
ULK+etch+H ₂	2.92±0.05	>40
ULK+etch+CH ₄	2.91±0.05	18
ULK+etch+O ₂	2.69±0.05	32

Previous workers have employed EP to characterize plasma-treated ULK films by using either methanol (18), or toluene and water (22), or by studying the solvent penetration kinetics (23). However the quantification of plasma-sealing strongly depends on the size of the probe molecule and the choice of the solvent is critical to determine the porosity of a plasma-treated film. The degree of plasma damage is also hard to determine because water vapors only partially condense into the modified part of the layer. In order to better understand the plasma impact, an EP analysis using a multi-solvent protocol has been systematically performed. As the pores can be modified during the treatment, methanol and toluene were used to compare the adsorption of molecules with a different size, and water was used to check the degree of plasma damage which is correlated to the hydrophilic volume properties of the layer (22). The ULK film after partial etching and

post-etching plasmas can be considered as a two-layer system with separate optical constants: a plasma-modified surface layer on top of a bulk undamaged ULK layer. However the small refractive index difference (less than 0.05) between the modified layer and the unmodified ULK cannot allow performing a reliable ellipsometric fit. Indeed, in the case of toluene and methanol, the condensation occurs into the modified layer as well as in the bulk unmodified ULK. Toluene and methanol measurements were therefore analyzed using a single layer model giving the whole porosity of the remaining film. On the contrary, the water condensation only occurs into the modified top layer due to its hydrophilicity, which leads to a significant change in refractive index. In that case, the EP measurements can be analyzed with a two-layer model if we assume the thickness and the optical properties of the undamaged bulk layer. Thus we can extract the properties of the hydrophilic pores in the modified layer.

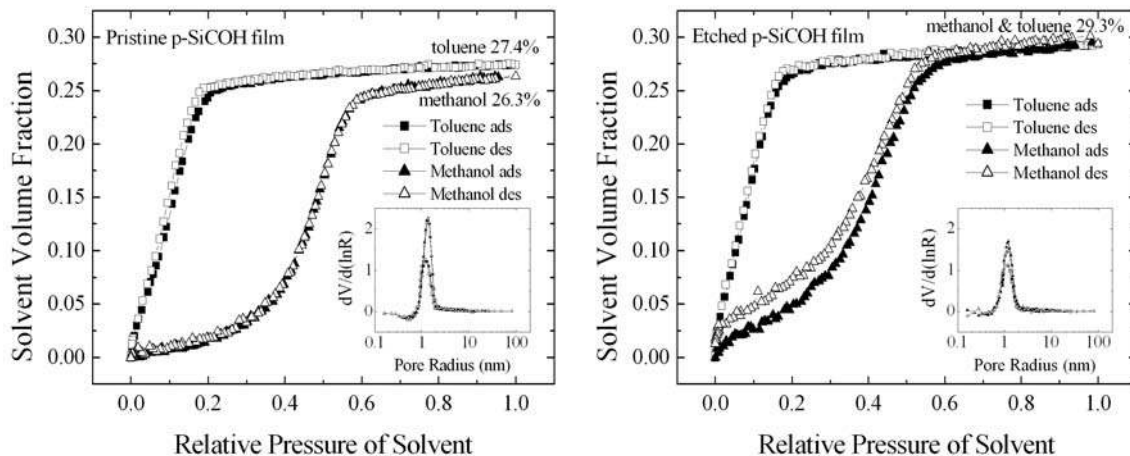


Figure 9. Toluene and methanol isotherms of pristine and etched p-SiCOH blanket films, inset: corresponding pore size distribution.

Figure 9 (left) shows, for the pristine ULK, the solvent volume fractions and pore size distributions obtained with toluene and methanol during the adsorption (ads) and desorption (des) sequences. The open porosity of the unmodified film is 27.4 % with toluene and 26.3 % with methanol, which values are close to the nominal 28 %. Pore size distributions for toluene and methanol give an average pore radius around 1.2 nm. EP results after partial etching are also presented in Figure 9 (right). The isotherms of toluene and methanol are quite similar to that of the pristine p-SiCOH and a porosity of 29.3 % is achieved considering a single layer model. The PSD calculation with both solvents gives the same values compared to the pristine p-SiCOH. The EP measurements with water, summarized in Table II, show that after etching, the water condenses partially into the modified layer (16% of porosity) indicating that only a few pores are hydrophilic. On the contrary, as the pristine material is hydrophobic, no porosity is detected with water. At last the etching plasma does not induce significant changes of porosity and pore size distribution of the remaining ULK film but involves a change of the hydrophobic properties of a part of the pores.

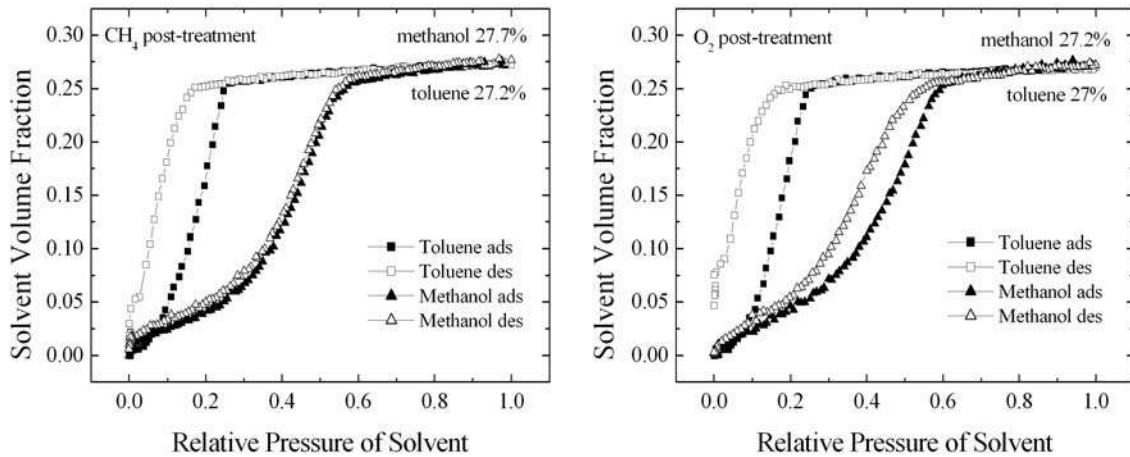


Figure 10. Toluene and methanol isotherms of CH_4 and O_2 post-treated p-SiCOH films.

EP results after the CH_4 and O_2 post-treatments are presented in Figure 10. In both cases the isotherm curves look similar to the unmodified sample with a porosity around 27 %. However we can notice the apparition of a small hysteresis in the case of CH_4 with toluene and in the case of O_2 with both toluene and methanol. As the pristine ULK measurement did not show this type of hysteresis, we can assume that the treatment slightly modifies the surface properties of the layer which changes the adsorption and desorption equilibrium conditions. In that case, the isotherm curves must be carefully interpreted and the corresponding PSD cannot be calculated. In addition, CH_4 and O_2 plasmas also lead to water condensation (Table II) into a fraction of the pores of the modified layer (12.3 % and 19.2 % respectively).

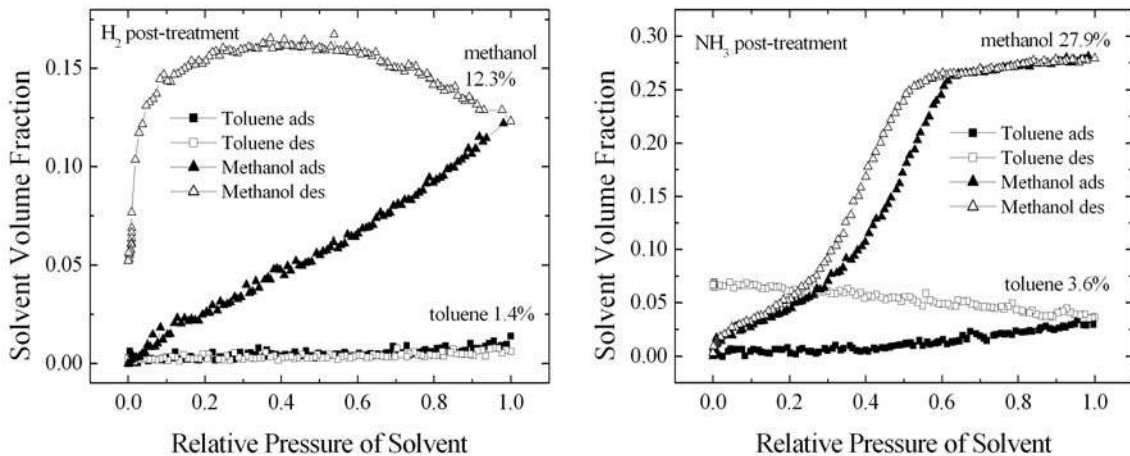


Figure 11. Toluene and methanol isotherms of H_2 and NH_3 post-treated p-SiCOH films.

EP results after H_2 post-treatment are presented in Figure 11 and Table II. As expected, this plasma treatment also induces p-SiCOH damage detected with water condensation in the modified layer (up to 16.7 %). However, the methanol adsorption curve does not have the typical plateau near the saturation vapor pressure indicating the total filling of the pores, and the desorption curve shows that the layer is still adsorbing methanol during the desorption. At the end of the desorption cycle, there is still around 5 % of methanol in the layer. In contrast to methanol, toluene (a bigger molecule) is no longer adsorbed after plasma (only 1.4 %). Those behaviors indicate a slow solvent

condensation kinetic. This is due to the densification of the surface which acts as a membrane. The filling time of the pores will depend on the molecule size and the solvent polarity and viscosity. In our experiments the dwell time between each pressure which is lower than one minute is not sufficient to reach the equilibrium condensation conditions that guarantee the complete filling of the pores. The dwell time should be adapted to each plasma-treated material but it is not predictable and in some cases it can become too long to make comfortable EP measurements. To a lesser extent, a similar behavior is observed after the NH_3 post-treatment. The modified layer is also partially hydrophilic (water content up to 10.2 %) and almost acts as a membrane for the toluene with a slow adsorption and desorption condensation kinetic. Methanol adsorption and desorption isotherms are still reversible but present a hysteresis loop and they reach the nominal open porosity of 27.9 %. In the end, all these measurements give useful information when integrating ULK materials about the surface modification but the results must be carefully interpreted because the isotherms are not acquired in equilibrium conditions. For example the PSD cannot be accurately calculated in these conditions and the porosity may be wrong in some cases because of a delayed solvent adsorption.

TABLE II. Porosimetry results of p-SiCOH blanket samples.

Porous films	Toluene	Methanol	Water uptake (%) in the modified layer
ULK (pristine)	Correct isotherms	Correct isotherms	0
ULK+etch	Correct isotherms	Correct isotherms	16
ULK+etch+ NH_3	Slow adsorption	Delayed adsorption	10.2
ULK+etch+ H_2	Slow adsorption	Slow adsorption	16.7
ULK+etch+ CH_4	Delayed adsorption	Delayed adsorption	12.3
ULK+etch+ O_2	Delayed adsorption	Delayed adsorption	19.2

In order to compare more precisely the membrane properties of the plasma-induced modified layers, we have performed EP kinetic measurements (23). Instead of monitoring the change of refractive index versus the relative pressure, the adsorptive relative pressure is quickly increased from the residual vacuum to 80% of the saturation pressure and the measurements are done versus time. At such a relative pressure, the measurements done on the pristine ULK film (Figure 9) show that the capillary condensation has already occurred and all the pores are filled. The kinetic measurements have been performed on blanket films with methanol and toluene (Figure 12). As expected the CH_4 , O_2 and NH_3 post-treatments show a methanol condensation kinetic nearly similar to the partially etched material which is well correlated with the solvent introduction in the chamber. At this relative pressure all the pores are quasi instantly filled due to the capillary condensation. However a small adsorption delay up to 2 min is measured between the partially etched and the post-treated films. This can be attributed to a densification of the surface that prevents the solvent adsorption. After the H_2 plasma treatment, the layer is filled after 240 min indicating a strong densification of the top surface. With the toluene, a higher delay is observed after the NH_3 and H_2 plasma treatments, respectively 250 and 1300 min, which indicates that the modified layer acts as a membrane. The whole results show that 1) after O_2 and CH_4 plasmas, the modified layer does not prevent the solvents diffusion, 2) after NH_3 plasma, the modified layer can be considered as a membrane and 3) the H_2 plasma treatment leads to a quasi pore sealing. The time to reach the plateau (equilibrium state of the adsorptive) is always higher with the toluene than with the methanol which indicates a slower diffusion kinetic mainly due

to a bigger molecular diameter. We also noticed that after all the post-treatments the value of the porosity is about 28 % which is the porosity of the pristine ULK material. This value is not always achieved with the EP measurements versus relative pressure because of an insufficient stabilization time. Those results show that only the surface is modified and there is no significant change of porosity in the remaining ULK material compared to the pristine ULK regardless of the plasma treatments.

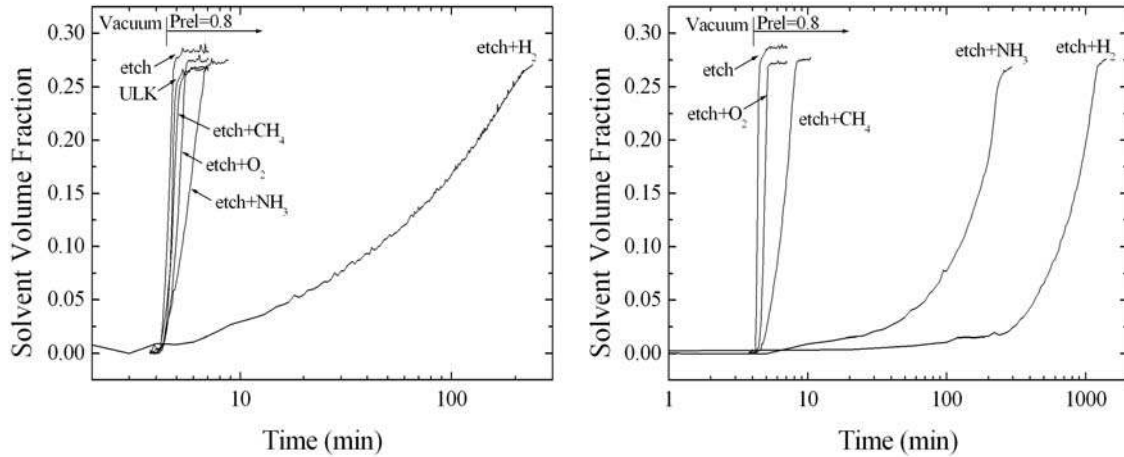


Figure 12. Methanol (left) and toluene (right) penetration kinetics of etched and post-treated p-SiCOH films.

Effect of plasma processes versus sample geometry

In order to compare EP and SP we have exposed a blanket porous film and a masked porous stack to similar etching plasma. After partial etching, the remaining blanket film has been analyzed with EP (Figure 9). After etching of the masked porous stack, a patterned structure is obtained (Figure 2). It consists of periodic lines of titanium nitride on top of an oxide capping layer and the p-SiCOH dielectric material. This grating has been analyzed by means of SP with the geometry described in Figure 13. The corresponding solvent volume fraction and pore size distribution obtained with methanol are shown in Figure 13. The pore size distribution is also centered on 1.2 nm and the open porosity is 27.8% which is a little smaller than the blanket film. However the two p-SiCOH were deposited on separate wafers with different thicknesses which may cause small discrepancies. In addition isotherms are consistent with those obtained on the blanket film with EP. Nevertheless SP isotherms show less hysteresis effects indicating a limited surface modification of the sidewalls during the etching step. These first SP results show that the technique is able to measure the porous properties of patterned structures and also to detect small differences between blanket and patterned structures.

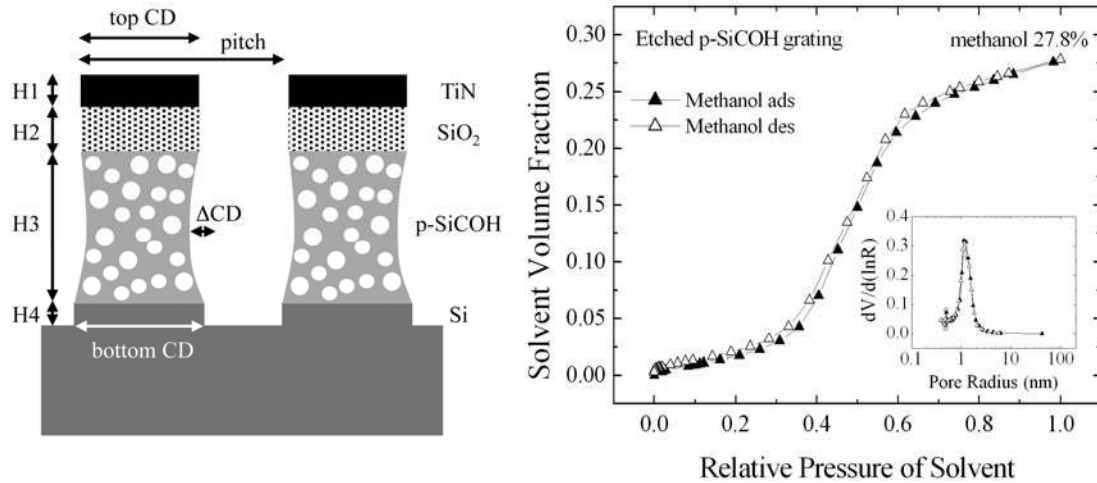


Figure 13. Left: definition of the parameterized geometrical parameters for the p-SiCOH grating. Right: methanol isotherms and PSD of the etched p-SiCOH grating.

In order to compare the sensitivity of horizontal and vertical porous surfaces to plasma treatments we have performed SP kinetic measurements with methanol. We have exposed patterned structures to the same NH_3 , H_2 , CH_4 , or O_2 based plasma treatments. The SP kinetic measurements were done on different gratings with the same geometry $\text{CD}=180$ nm and $\text{pitch}=340$ nm. Solvent volume fraction results are presented in Figure 14. Unlike previous thin films results, all the post-treatments present a fast methanol condensation kinetic (less than 30 s) indicating a reduced diffusion barrier. This can be explained by the vertical geometry of the sidewalls which are less exposed to ion bombardment during the plasma processes. These differences between blanket and patterned films highlight the interest of the technique for real interconnect process monitoring. EP measurements on blanket films may not be fairly representative of plasma-induced modifications on vertical structures.

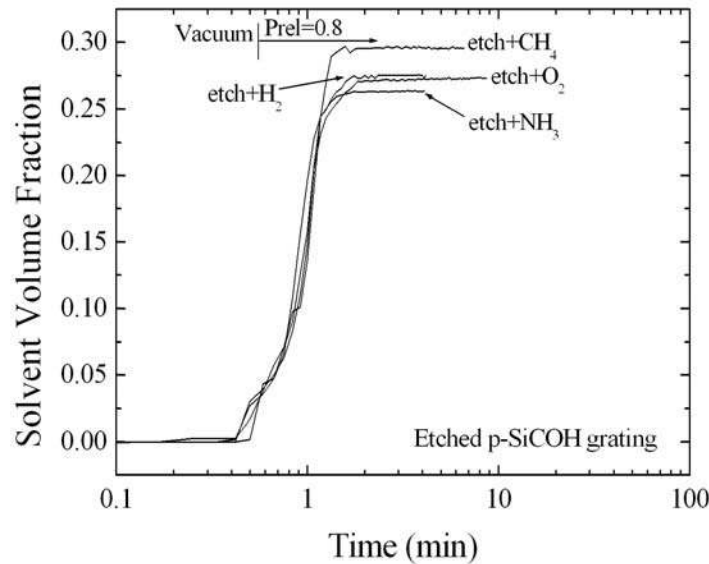


Figure 14. Methanol penetration kinetics of etched and post-treated p-SiCOH gratings.

Finally SP measurements were also performed using water as solvent to detect any change of the ULK hydrophobic properties. Two gratings were prepared using the standard etching process and post-treated with either capacitive O₂ plasma (FLEX45DDTM) or O₂ downstream plasma. SP results considering a scatterometric model with a uniform porous material are shown in Figure 15. As expected water condensation clearly occurs after the O₂ downstream plasma because of the full methyl group depletion. The measured porosity is close to the pristine film value indicating that almost all the pores are hydrophilic. On the contrary the O₂ post-treatment allows a small amount of water to be condensed (7.6%). In that case, water only condensates in the pores located near the sidewall surface which is modified by the plasma. The small hysteresis observed in that case is linked to surface modifications which prevent water to be adsorbed in the same conditions than in uniform hydrophilic samples. Through SP with water vapors, it is therefore possible to detect the plasma-induced damage of porous materials as integrated in a structure.

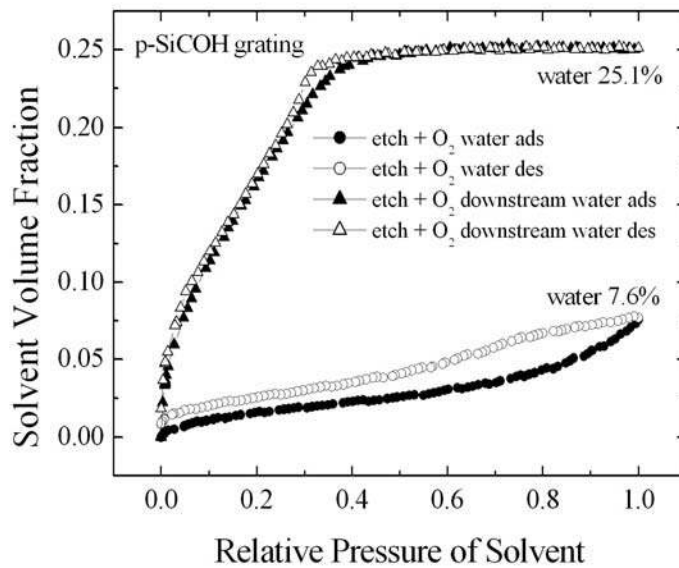


Figure 15. Water isotherms of O₂ and O₂ downstream post-treated p-SiCOH gratings.

The quantification of plasma-induced damage could also be possible through SP. However it adds more complexity to the model and therefore more correlation issues. Indeed the refractive index of modified sidewalls when the pores are empty is close to the bulk p-SiCOH then it is not possible to define directly a geometric model with modified sidewalls. However as we know the refractive index of the hydrophilic material filled with water from previous measurements after O₂ downstream plasma, it is possible to model a structure by varying the sidewall thickness and keeping constant the refractive index of the fully hydrophilic material. The thickness value found at saturation pressure will therefore be equivalent to the modified sidewall thickness with the assumption that all the pores of the modified layer are hydrophilic. We have compared this complex geometric modeling to the conventional decoration method. In this method cleaved patterned samples are exposed to 1% diluted HF for 15 s. Indeed the damaged layer is quickly removed by the HF solution, while the unmodified material is hardly consumed. The trenches are filled with resist prior to the HF dip to prevent potential collapse of features during SEM exposure (Figure 16). The comparison of the modified layer thickness estimated with both techniques is shown in Figure 17. Similar thicknesses are

observed with both techniques except after the etching plasma but the SEM measurement has a worse accuracy than scatterometry. We found that the thickness of the modified sidewall depends on the post-treatment plasma. In conclusion plasma modifications were observed for both horizontal and vertical geometries regardless of the plasma treatments. In addition to plasma modifications, surface densification was also observed in the bottom of the trench which is more exposed to ion bombardment.

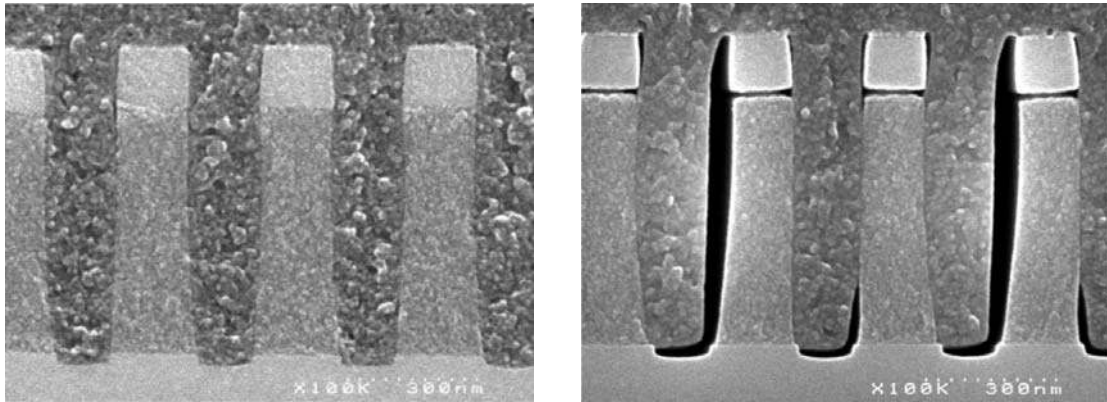


Figure 16. SEM cross-sections of plasma-treated p-SiCOH gratings before (left) and after (right) HF dip.

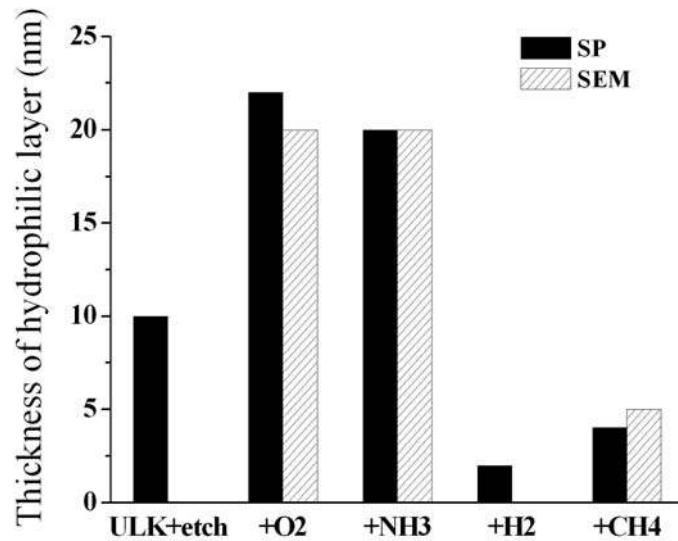


Figure 17. Estimation of the plasma-modified thickness of a porous grating with SP and decoration technique.

Conclusion

The properties of porous materials need to be assessed during their integration in CMOS interconnect levels. In the dual damascene architecture, plasma-induced modifications of porous materials are likely to occur in the bottom of the trench and in the sidewall regions, i.e. respectively in horizontal and vertical geometry. We have used Ellipsometric Porosimetry with a multi-solvent protocol and a kinetic measurement mode on plasma-treated blanket films to replicate the bottom of the trenches. No significant

changes of porosity and pore size were evidenced in the remaining ULK film regardless of the plasma. However surface modifications such as densification and hydrophilization are observed. The modified layers induced by the etching plasma, the O₂, and the CH₄ based plasmas do not prevent the solvent condensation. On the contrary the modified layers induced by the NH₃, and the H₂ based plasmas act as a membrane which slows down the condensation kinetic and leads to a quasi pore sealing. We have used the recently developed Scatterometric Porosimetry technique to characterize the sidewall of patterned structures. One advantage of SP is that it can be implemented with an already existing EP tool using a specific modeling procedure. However SP measurements must be done on periodic structures which have to be equivalent to the real circuit in terms of dimensions and stack. We have performed a side-by-side comparison between EP and SP on different plasma-treated samples using the same multi-solvent and kinetic protocols. The results showed that the effect of plasma processes is different on patterned structures compared with blanket films. In particular, different surface densification is observed highlighting that porous material modifications strongly depend on the sample geometry. Such a characterization technique is expected to be useful for microelectronic applications on patterned wafers as it is a potential technique to characterize sidewall damage after each step of the etch process. It also appears as a good complementary technique to EP which only provides quantitative measurements on continuous layers.

References

1. N. Posseme, T. Chevolleau, T. David, M. Darnon, O. Louveau, O. Joubert, *J. Vac. Sci. Technol. B*, **25**, 1928 (2007).
2. N. Posseme, T. Chevolleau, R. Bouyssou, T. David, V. Arnal, J. P. Barnes, C. Verove, and O. Joubert, *J. Vac. Sci. Technol. B*, **28**, 809 (2010).
3. F. Bailly, T. David, T. Chevolleau, M. Darnon, N. Posseme, R. Bouyssou, J. Ducote, O. Joubert, and C. Cardinaud, *J. Appl. Phys.*, **108**, 014906 (2010).
4. M. Darnon, T. Chevolleau, D. Eon, R. Bouyssou, B. Pelissier, L. Vallier, O. Joubert, N. Posseme, T. David, F. Bailly, and J. Torres, *Microelectron. Eng.*, **85**, 2226 (2008).
5. M.R. Baklanov, K.P. Mogilnikov, V.G. Polovinkin, F.N. Dultsev, *J. Vac. Sci. Technol. B*, **18**, 1385 (2000).
6. Patent pending No. FR 09 55027.
7. R. Bouyssou, M. El Kodadi, C. Licitra, T. Chevolleau, M. Besacier, N. Posseme, O. Joubert, and P. Schiavone, *J. Vac. Sci. Technol. B*, **28**, L31 (2010).
8. N. Posseme, T. Chevolleau and R. Bouyssou, T. David, V. Arnal, M. Darnon, Ph. Brun, C. Verove, O. Joubert, *J. Vac. Sci. Technol. B*, **29**, in press (2010).
9. C. Licitra, R. Bouyssou, T. Chevolleau, F. Bertin, *Thin Solid Films*, **518**, 5140 (2010).
10. A. Bourgeois, Y. Turcant, C. Walsh, C. Defranoux, *J.-J. Int. Adsorp. Soc.*, **14**, 457 (2008).
11. H. Kleinknecht, H. Meier, *Appl. Opt.*, **19**, 525 (1980).
12. Fujiwara, H., Principles of Optics, in *Spectroscopic Ellipsometry: Principles and Applications*, John Wiley & Sons, Ltd, Chichester, UK (2007).
13. L. Li, C. W. Haggans, *J. Opt. Soc. Am. A*, **10**, 1184 (1993).
14. M. El Kodadi, S. Soulan, M. Besacier, and P. Schiavone, *J. Vac. Sci. Technol. B*, **27**, 3232 (2009).

15. Fujiwara, H., Data Analysis, in *Spectroscopic Ellipsometry: Principles and Applications*, John Wiley & Sons, Ltd, Chichester, UK (2007).
16. A.W. Adamson, A.P. Gast, *Physical Chemistry of Surfaces*, John Wiley & Sons, New York (1997).
17. P. Revol, D. Perret, F. Bertin, F. Fusalba, V. Rouessac, A. Chabli, G. Passemard, *J. Porous Mater.*, **12**, 113 (2005).
18. N. Posseme, T. Chevolleau, T. David, M. Darnon, J.P. Barnes, O. Louveau, C. Licitra, D. Jalabert, H. Feldis, M. Fayolle, O. Joubert, *Microelectron. Eng.*, **85**, 1842 (2008).
19. K. Maex, M.R. Baklanov, D. Shamiryan, F. Iacopi, S.H. Brongersma, Z.S. Yanovitskaya, *J. Appl. Phys.*, **93**, 8793 (2003).
20. A. Grill, V. Sternhagen, D. Neumayer, V. Patel, *J. Appl. Phys.*, **98**, 074502 (2005).
21. Q.T. Le, M.R. Baklanov, E. Kesters, A. Azioune, H. Struyf, W. Boullart, J.J. Pireaux, S. Vanhaelemeersch, *Electrochem. Solid-State Lett.*, **8**, F21 (2005).
22. M.R. Baklanov, K.P. Mogilnikov, Q.T. Le, *Microelectron. Eng.*, **83**, 2287 (2006).
23. W. Puyrenier, V. Rouessac, L. Broussous, D. Rébiscoul, A. Ayrat, *Microporous Mesoporous Mater.*, **106**, 40 (2007).